Graphite-Conjugation Enhances Porphyrin Electrocatalysis

Corey J. Kaminsky,[†] Joshua Wright,[‡,§] and Yogesh Surendranath*,[†]

[†]Department of Chemistry, Massachusetts Institute of Technology, Cambridge, Massachusetts 02139, United States
[‡]Advanced Photon Source, Argonne National Laboratory, 9700 Cass Avenue, Lemont, Illinois 60439, United States
[§]Illinois Institute of Technology, 3300 South Federal Street, Chicago, Illinois 60616, United States

Ⓢ *Supporting Information*

ABSTRACT: We synthesize porphyrins that are strongly electronically coupled to carbon electrodes by condensing diaminoporphyrin derivatives onto *o*-quinone moieties native to graphitic carbon surfaces. X-ray photoelectron and absorption spectroscopies along with electrochemical data establish the formation of a high-fidelity conjugated pyrazine linkage to the surface with preservation of the metalloporphyrin scaffold. Using the O_2 reduction reaction (ORR) as a probe, we find that conjugation dramatically enhances the rate of catalysis. A graphite-conjugated Co porphyrin, GCC-CoTPP, displays an onset current density of 10 $\mu A/cm^2$ at 0.72 V versus the reversible hydrogen electrode, whereas a nonconjugated amide-linked Co porphyrin onsets at 0.66 V. This corresponds to an order of magnitude enhancement in the activation-controlled turnover frequencies for ORR upon conjugation. This work establishes a versatile platform for examining the emergent reactivity of porphyrins strongly coupled to metallic electrodes.

KEYWORDS: *molecular electrocatalysis, heterogeneous electrocatalysis, oxygen reduction, porphyrin, supported catalysts, electron transfer*
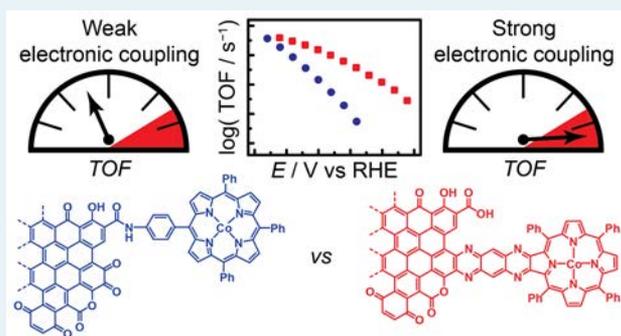
Porphyrins are ubiquitous active sites that catalyze a wide array of multielectron electrochemical transformations. In particular, they are known to be active for the O_2 reduction reaction,[1−4] the reduction of CO_2,[3,5] the evolution of H_2,[2,3] and the oxidation of small molecules including alcohols.[3,4,6,7] Translating the rich chemistry of porphyrins to practical energy conversion devices requires high-fidelity strategies for modifying electrode surfaces with porphyrin active sites.

Although a wide array of strategies have been developed for attaching porphyrins to electrode surfaces,[8,9] the impact of the linkage chemistry on the performance of the resulting electrode remains largely unknown. Importantly, careful studies of porphyrin-modified electrodes reveal that the same porphyrin active site can exhibit vastly disparate activity depending on the preparation of the electrode substrate, the method of surface ligation, and ancillary constituents of the modified electrode.[10−12] These studies imply that the electronic interaction of the porphyrin with the surface and the local chemical environment at the active site play an outsized role in defining the catalytic activity of the porphyrin-modified electrode. Although diverse strategies have been employed to tune the local environment of the porphyrin active site,[13−17] the impact of electronic coupling to the electrode surface has been underexplored as a method for promoting catalysis.

We have developed a high-fidelity chemistry for attaching molecules to graphitic carbon surfaces through robust aromatic pyrazine linkages.[18−21] These graphite-conjugated catalysts (GCCs) are prepared by condensation of an organic 1,2-diamine with *ortho*-quinone moieties native to graphitic carbon surfaces.[18] The strong electronic coupling provided by this linkage radically alters the electron transfer properties of the molecular unit. In particular, the strong coupling excludes metal-centered redox cycling via outer-sphere electron transfer and ensures that electron flow is concerted with substrate bond activation.[21] As a result, GCCs do not exhibit outer-sphere redox events typical of weakly coupled surface-ligated molecules but instead possess the interfacial electron transfer properties of metallic surface sites.[21] Thus, GCCs provide an ideal platform for directly probing the impact of electronic coupling on the activity of the bound catalyst. Herein, we develop a general strategy to conjugate porphyrin scaffolds to graphitic carbon surfaces. Using a graphite-conjugated cobalt porphyrin and the O_2 reduction reaction as a test case, we demonstrate that the strong electronic coupling enabled by conjugation confers dramatically enhanced catalytic activity relative to a more weakly coupled amide-linked cobalt porphyrin. This work establishes the critical role of electronic coupling in defining the catalytic activity of porphyrin-modified electrodes and enables the exploration of the rich chemistry of porphyrins strongly coupled to metallic surfaces.

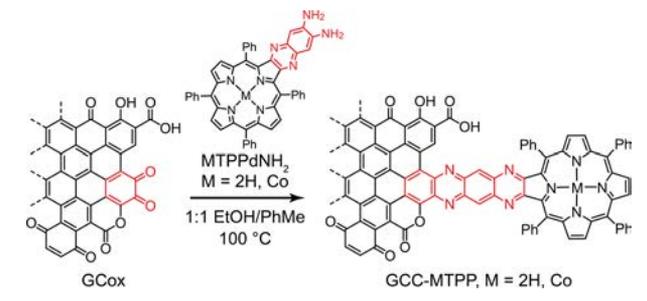A suitable diamine-containing porphyrin synthon, $H_2TPPdNH_2$ ($TPPdNH_2$ = 5,10,15,20−tetraphenyl-6′,7′-diaminoquinoxalino[2,3-b′]porphyrin) (Scheme 1),[22,23] was

Scheme 1. Synthesis of GCC-MTPP Active Sites

Figure 1. Characterization of GCC-CoTPP by X-ray photoelectron spectroscopy, X-ray absorption spectroscopy, and cyclic voltammetry. (a) High-energy resolution XPS scan of the N 1s region. Measured signal is in gray, fit peaks in red, background and overall fit peak envelope in black. (b) High-energy resolution XPS scan of the Co 2p region. Measured signal is in gray and fit peaks in black. (c) Extended X-ray absorption fine structure of GCC-CoTPP and model complexes. (d) Cyclic voltammogram of GCC-CoTPP under N_2 in 0.1 M NaOH recorded at 10 mV/s scan rate. Initial direction of scan indicated on plot.

accessed via a modified literature procedure that is fully described in the Supporting Information. Metalation in the presence of $Co(OAc)_2 \cdot 4H_2O$ yields $CoTPPdNH_2$. Washing an organic solution of $CoTPPdNH_2$ with an aqueous solution of ethylenediaminetetraacetic acid does not result in demetalation, suggesting that the metal is chelated in the central cavity rather than at the peripheral diamine.[24] The UV−vis spectrum shows a coalescence of the four Q-band peaks of $H_2TPPdNH_2$ into two broad peaks for $CoTPPdNH_2$ and a blue shift of the Soret band of $CoTPPdNH_2$ relative to $H_2TPPdNH_2$, both consistent with chelation of cobalt by the porphyrin macrocycle.[25] GCCs were prepared by exposing a preoxidized glassy carbon surface (GCox) to the diamine porphyrin precursor in a 1:1 EtOH/Toluene solution at 100 °C. Electrodes were then soaked in toluene followed by 0.1 M HCl to liberate phyisisorbed and monoimine linked porphyrins from the surface.[18] The resulting surfaces are denoted as GCC-MTPP (M = 2H, Co) (Scheme 1).

X-ray photoelectron spectroscopy (XPS) evinces incorporation of the porphyrin units onto the surface of the GCox substrate. Survey analysis reveals the appearance of N 1s peaks in the spectra of GCC-MTPP (Figures S1 and S2). For GCC-CoTPP, we observe Co 2p peaks that integrate to yield a N:Co atomic ratio of 8.2:1, consistent with the expected ratio of 8:1 for GCC-CoTPP. High-resolution scans of the N 1s region reveal a feature that deconvolutes into two peaks in a 1:1 ratio for both GCC-CoTPP (Figure 1a) and GCC-H$_2$TPP (Figure S3). We assign the peak centered at 398.4 eV as pyrrolic N based on comparison with cobalt meso-tetraphenylporphine (CoTPP) and CoTPPdNH$_2$, which display N 1s XPS peaks at 398.8 and 398.4 eV, respectively (Figures S4 and S5). We assign the broad peak centered at 399.8 eV to pyrazinic N based on comparison to the observed value of 399.7 eV for CoTPPdNH$_2$. The large fwhm of the pyrazinic N reflects the varied local environments present on the carbon surface and/or the presence of two unique pyrazine moieties per GCC-CoTPP site. Notably, the GCC-CoTPP spectrum does not show a significant peak near 401.3 eV, which corresponds to the protonated amines of CoTPPdNH$_2$ (Figure S5). High-resolution scans of the Co 2p region for GCC-CoTPP (Figure 1b) resolve the $2p_{3/2}$ and $2p_{1/2}$ doublet at 779.9 and 795.2 eV, respectively, consistent with literature values for CoTPP.[26] Taken together, the XPS data support the formation of isolated CoTPP sites conjugated to the surface via pyrazine linkages.

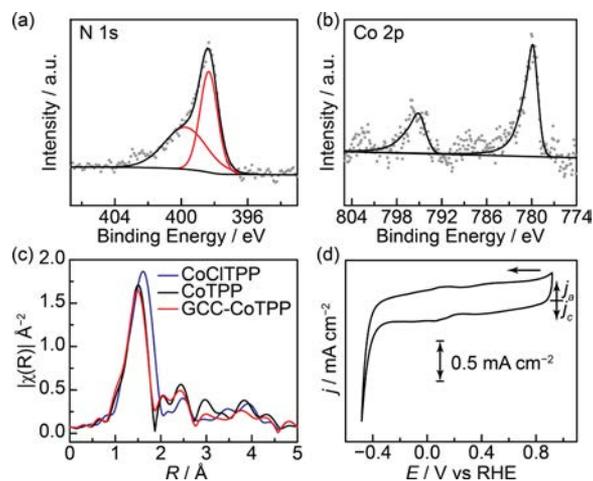To further characterize the local coordination environment and electronic structure of the Co center in GCC-CoTPP, we collected X-ray absorption spectroscopy (XAS) measurements on functionalized high-surface area carbons (see SI for synthetic details). The extended X-ray absorption fine structure (EXAFS) spectrum of GCC-CoTPP (Figure 1c, red) is very similar to that of CoTPP (Figure 1c, black) indicating the preservation of the square planar coordination environment. Although exposure to aerobic HCl leads to conversion of CoTPP to CoClTPP,[27] our aerobic HCl wash of the surface (see above) does not lead to the same conversion for GCC-CoTPP. Indeed, EXAFS spectra exclude the presence of an axial Cl ligand in GCC-CoTPP; the first shell scattering peak for GCC-CoTPP (Figure 1c, red) does not display the enhanced intensity or R-value shift observed for the CoClTPP standard (Figure 1c, blue). Interestingly, the X-ray absorption near-edge spectrum (XANES) of GCC-CoTPP reveals pre-edge features consistent with the presence of both Co(II) and Co(III) in a porphyrin coordination environment (Figure S6), despite a dominant square-planar coordination environment. Together, the data suggest that while conjugation may serve to alter the local electronic structure of the Co centers on the surface, it nonetheless preserves their local coordination environment.

Quantitative information about the surface concentration of the conjugated Co center is provided by a combination of cyclic voltammetry and inductively coupled plasma mass spectrometry (ICP-MS). Cyclic voltammograms (CVs) of modified electrodes display broad surface redox waves centered at 0.1 V (all potentials are reported vs the reversible hydrogen electrode (RHE)) for both GCC-CoTPP (Figure 1d) and GCC-H$_2$TPP (Figure S7). We assign this surface wave to the 2e$^-$/2H$^+$ reduction of the surface pyrazine units to dihydropyrazine, consistent with previous observations of other GCCs.[18,19,21] Given the propensity of physisorbed CoTPP units to rapidly desorb from GCox under potential cycling (Figure S8), the integration of this wave provides an in situ and nondestructive measurement of the surface concen-

tration of Co active sites that are conjugated to the electrode. To independently calibrate this method, we compared Co surface concentrations determined by ICP-MS of acid digested electrodes to the pyrazine wave integration and found an e^--to-Co ratio of 1.80 ± 0.11 (see SI for details). This value implies that both pyrazine moieties in the linker give rise to a single $2e^-/2H^+$ redox process per surface porphyrin unit. Using this integer charge-to-Co ratio, we used the integration of the surface redox wave to quantify, in situ, the surface concentration of Co sites and find a value of 2.2 ± 0.2 nmol/cm^2 for the electrodes used in all subsequent studies. Together, the ICP-MS and electrochemical data corroborate the XAS and XPS data to establish that this synthetic procedure furnishes surface porphyrins that are conjugated to carbon electrodes.

To probe the catalytic potential of the GCC-porphyrin scaffold, we chose the kinetically demanding oxygen reduction reaction (ORR). Although a wide array of molecular metalloporphyrins have been exhaustively investigated for ORR catalysis,[1−4,28,29] our studies constitute the first investigations of porphyrins strongly coupled to carbon surfaces. Indeed, we find that GCC-CoTPP is a highly active catalyst for the ORR in acidic media. Polarization of GCC-CoTPP under an atmosphere of N_2 in 0.1 M $HClO_4$ (Figure 2,
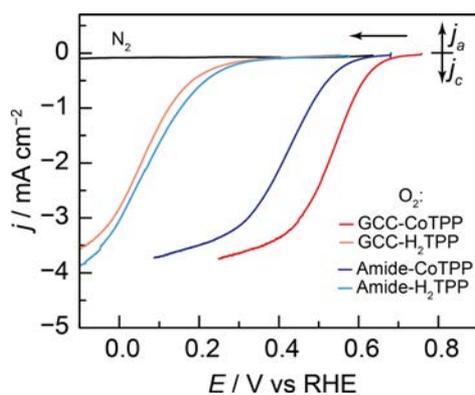

Figure 2. Linear sweep voltammograms (LSVs) of GCC-CoTPP (red), amide-linked CoTPP (dark blue), GCC-H$_2$TPP (orange), amide-linked H$_2$TPP (sky blue), and GCox (gray) recorded under an O_2 atmosphere. LSV of GCC-CoTPP under an N_2 atmosphere (black). All data were recorded in 0.1 M HClO$_4$ at a 5 mV/s scan rate with the electrode rotated at 2000 rpm.

black) shows current associated with double layer charging and the $2e^-/2H^+$ reduction of the pyrazine linkages. In the presence of 1 atm of O_2, GCC-CoTPP electrodes display a large catalytic wave with an onset current density of 10 μA/cm^2 at 0.72 V (Figure 2, red). The catalytic wave begins to plateau at ~0.42 V due to the onset of transport limitations. In contrast, GCC-H$_2$TPP displays the same ORR activity as that of an unmodified GCox electrode (Figure 2, orange and gray). Together, the data indicate that the GCC-CoTPP is a potent ORR catalyst and that the Co center is the active site for O_2 reduction in acidic media.

To determine the impact of conjugation on catalytic activity, we benchmarked GCC-CoTPP against a nonconjugated, surface-ligated cobalt porphyrin. For this comparison, we chose to link the porphyrin to the surface through a *meso*-aryl connection because *meso*-aryl linkages are known to engender weak coupling in molecular porphyrin dyads.[30] Glassy carbon

electrodes were pretreated according to the GCC procedure, treated with thionyl chloride, and then exposed to cobalt 5-(*p*-aminophenyl)-10,15,20-triphenylporphine to furnish Amide-CoTPP (Scheme 2).[31−33] XPS evinces incorporation of the

Scheme 2. Synthesis of Amide-MTPP
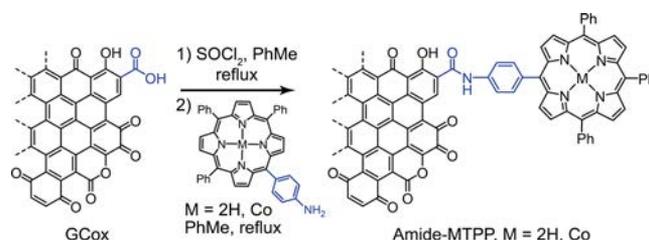
amide-linked cobalt porphyrin moiety onto the surface (Figure S9). Unlike for the GCC-CoTPP, there are no clear surface redox waves that can be used to quantify Co concentration in situ,[33] and thus, we used ICP-MS analysis of acid digested electrodes to estimate a surface Co concentration of 0.9 ± 0.5 nmol/cm^2 (see SI for details). An analogous procedure was used to prepare the corresponding Amide-H$_2$TPP as an additional control (see SI).

The catalytic activity of Amide-CoTPP is inferior to that of GCC-CoTPP. Under an O_2 atmosphere, the Amide-CoTPP (Figure 2, blue) displays significantly greater activity than that of Amide-H$_2$TPP (Figure 2, sky blue), indicating that the Co center mediates catalysis. However, the catalytic wave for Amide-CoTPP (Figure 2, blue) onsets with a current of 10 μA/cm^2 at 0.66 V, requiring 60 mV greater overpotential than GCC-CoTPP (Figure 2, red) under identical conditions. The enhanced activity of GCC-CoTPP is more clearly understood in a plot of per site turnover frequency (TOF) for the two systems (Figure 3). At high overpotentials beyond 0.55 V,
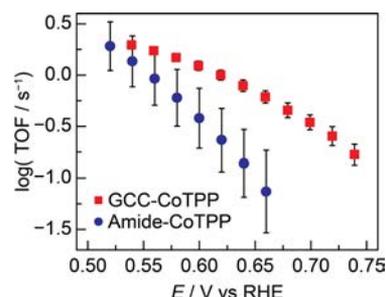

Figure 3. Turnover frequencies for the ORR as a function of potential for GCC-CoTPP (red) and Amide-CoTPP (blue). Error bars represent one standard deviation. The large error bars observed for the Amide-CoTPP arise from variation in the surface coverage, as evinced by the large error value indicated in the main text. All data were recorded in 0.1 M HClO$_4$ with the electrode rotated at 2000 rpm.

where the catalysts begin to experience significant transport limitations, the TOF for GCC-CoTPP (Figure 3, red) and Amide-CoTPP (Figure 3, blue) begin to converge to a similar value. However, at lower overpotentials, where the rate of catalysis is activation controlled, GCC-CoTPP (Figure 3, red) displays superior activity with nearly an order of magnitude improvement in TOF relative to the average value for Amide-CoTPP at 0.66 V (Figure 3, blue). Notably, the reaction selectivity is similar between the two systems. Koutecký−

Levich analysis reveals that GCC-CoTPP transfers 2.6 ± 0.2 electrons per O_2 reduced, whereas Amide-CoTPP transfers 2.4 ± 0.15 electrons per O_2 reduced (Figure S10). Given that peroxide/water branching is also governed by the rate of proton delivery to M-OOH intermediates,[14,34] it is unsurprising that the degree of electronic coupling has a minimal impact on selectivity relative to other factors such as the local pH environment. Nonetheless, the data establish that surface conjugation significantly enhances the rate of O_2 reduction catalysis. While detailed mechanistic studies are ongoing, we postulate that this enhancement derives from changes in the electron transfer and O_2 activation mechanism conferred by the strong electronic coupling engendered by graphite conjugation.

In summary, we have developed a general method for conjugating porphyrins to graphitic carbon surfaces. We find that GCC-CoTPP is a potent catalyst for ORR in acidic aqueous electrolyte and that conjugation dramatically enhances the activation controlled rate of the ORR at the Co site. This work establishes that the degree of electronic coupling to the surface is an important design consideration for maximizing the activity of the bound porphyrin unit. Given the abundance of metalloporphyrin complexes and their diverse reactivity manifolds, this work enables a broad exploration into the emergent reactivity of porphyrins strongly coupled to metallic surfaces across electrochemical and thermal transformations.

■ ASSOCIATED CONTENT

ⓢ Supporting Information

The Supporting Information is available free of charge on the ACS Publications website at DOI: 10.1021/acscatal.9b00404.

> Full experimental details, synthetic procedures, XPS data, XAS data, and additional electrochemical data (PDF)

■ AUTHOR INFORMATION

Corresponding Author
*E-mail: yogi@mit.edu.
ORCID ⬤
Yogesh Surendranath: 0000-0003-1016-3420

Notes
The authors declare the following competing financial interest(s): C.J.K. and Y.S. are inventors on patent application 15/236,963 submitted by the Massachusetts Institute of Technology that covers the graphite conjugated materials described in this work.

■ ACKNOWLEDGMENTS

■ REFERENCES

(1) Boulatov, R. Metalloporphyrin Catalysts of Oxygen Reduction. In *Fuel Cell Catalysis: A Surface Science Approach*; Koper, M. T. M., Wieckowski, A., Eds.; Wiley: Hoboken, NJ, 2009; pp 637−693.

(2) Zhang, W.; Lai, W.; Cao, R. Energy-Related Small Molecule Activation Reactions: Oxygen Reduction and Hydrogen and Oxygen Evolution Reactions Catalyzed by Porphyrin- and Corrole-Based Systems. *Chem. Rev.* 2017, 117, 3717−3797.

(3) Zagal, J. H.; Griveau, S.; Silva, J. F.; Nyokong, T.; Bedioui, F. Metallophthalocyanine-Based Molecular Materials as Catalysts for Electrochemical Reactions. *Coord. Chem. Rev.* 2010, 254, 2755−2791.

(4) Lemon, C. M.; Dogutan, D. K.; Nocera, D. G. Porphyrin and Corrole Platforms for Water Oxidation, Oxygen Reduction, and Peroxide Dismutation. In *The Porphyrin Handbook*; Kadish, K. M., Smith, K. M., Guilard, R., Eds.; Academic Press: San Diego, 2000; Vol. 21; pp 1−143.

(5) Manbeck, G. F.; Fujita, E. A Review of Iron and Cobalt Porphyrins, Phthalocyanines and Related Complexes for Electrochemical and Photochemical Reduction of Carbon dioxide. *J. Porphyrins Phthalocyanines* 2015, 19, 45−64.

(6) Meunier, B. Metalloporphyrins as Versatile Catalysts for Oxidation Reactions and Oxidative DNA Cleavage. *Chem. Rev.* 1992, 92, 1411−1456.

(7) *Metalloporphyrins in Catalytic Oxidations*; Sheldon, R. A., Ed.; Marcel Dekker, Inc.: New York, 1994.

(8) Duclairoir, F.; Marchon, J.-C. Anchoring of Porphyrins and Phthalocyanines on Conductors and Semi-Conductors for Hybrid Electronics. In *The Porphyrin Handbook*; Kadish, K. M., Smith, K. M., Guilard, R., Eds.; Academic Press: San Diego, 2000; Vol. 10; pp 245−311.

(9) Griveau, S.; Bedioui, F. Electropolymerized Thin Films of Metalloporphyrins for Electrocatalysis and Electroanalysis. In *The Porphyrin Handbook*; Kadish, K. M., Smith, K. M., Guilard, R., Eds.; Academic Press: San Diego, 2000; Vol. 12; pp 227−295.

(10) Rigsby, M. L.; Wasylenko, D. J.; Pegis, M. L.; Mayer, J. M. Medium effects are as Important as Catalyst Design for Selectivity in Electrocatalytic Oxygen Reduction Iron-Porphyrin Complexes. *J. Am. Chem. Soc.* 2015, 137, 4296−4299.

(11) Morozan, A.; Campidelli, S.; Filoramo, A.; Jousselme, B.; Palacin, S. Catalytic Activity of Cobalt and Iron Phthalocyanines or Porphyrins Supported on Different Carbon Nanotubes towards Oxygen Reduction Reaction. *Carbon* 2011, 49, 4839−4847.

(12) Birdja, Y. Y.; Vos, R. E.; Wezendonk, T. A.; Jiang, L.; Kapteijn, F.; Koper, M. T. M. Effects of Substrate and Polymer Encapsulation on CO_2 Electroreduction by Immobilized Indium(III) Protoporphyrin. *ACS Catal.* 2018, 8, 4420−4428.

(13) Azcarate, I.; Costentin, C.; Robert, M.; Savéant, J.-M. Through-Space Charge Interaction Substituent Effects in Molecular Catalysis Leading to the Design of the Most Efficient Catalyst of CO_2-to-CO Electrochemical Conversion. *J. Am. Chem. Soc.* 2016, 138, 16639−16644.

(14) McGuire, R., Jr.; Dogutan, D. K.; Teets, T. S.; Suntivich, J.; Shao-Horn, Y.; Nocera, D. G. Oxygen Reduction Reactivity of Cobalt(II) Hangman Porphyrins. *Chem. Sci.* 2010, 1, 411−414.

(15) Ye, L.; Fang, Y.; Ou, Z.; Xue, S.; Kadish, K. M. Cobalt Tetrabutano- and Tetrabenzotetraarylporphyrin Complexes: Effect of Substituents on the Electrochemical Properties and Catalytic Activity

of Oxygen Reduction Reactions. *Inorg. Chem.* **2017**, *56*, 13613−13626.

(16) Collman, J. P.; Wagenknecht, P. S.; Hutchison, J. E. Molecular Catalysts for Multielectron Redox Reactions of Small Molecules: The "Cofacial Metallodiporphyrin" Approach. *Angew. Chem., Int. Ed. Engl.* **1994**, *33*, 1537−1554.

(17) Pegis, M. L.; McKeown, B. A.; Kumar, N.; Lang, K.; Wasylenko, D. J.; Zhang, X. P.; Raugei, S.; Mayer, J. M. Homogenous Electrocatalytic Oxygen Reduction Rates Correlate with Reaction Overpotential in Acidic Organic Solutions. *ACS Cent. Sci.* **2016**, *2*, 850−856.

(18) Fukushima, T.; Drisdell, W.; Yano, J.; Surendranath, Y. Graphite-Conjugated Pyrazines as Molecularly Tunable Heterogeneous Electrocatalysts. *J. Am. Chem. Soc.* **2015**, *137*, 10926−10929.

(19) Oh, S.; Gallagher, J. R.; Miller, J. T.; Surendranath, Y. Graphite-Conjugated Rhenium Catalysts for Carbon Dioxide Reduction. *J. Am. Chem. Soc.* **2016**, *138*, 1820−1823.

(20) Ricke, N. D.; Murray, A. T.; Shepherd, J. J.; Welborn, M. G.; Fukushima, T.; Van Voorhis, T.; Surendranath, Y. Molecular-Level Insights into Oxygen Reduction Catalysis by Graphite-Conjugated Active Sites. *ACS Catal.* **2017**, *7*, 7680−7687.

(21) Jackson, M. N.; Oh, S.; Kaminsky, C. J.; Chu, S. B.; Zhang, G.; Miller, J. T.; Surendranath, Y. Strong Electronic Coupling of Molecular Sites to Graphitic Electrodes via Pyrazine Conjugation. *J. Am. Chem. Soc.* **2018**, *140*, 1004−1010.

(22) Crossley, M. J.; Govenlock, L. J.; Prashar, J. K. Synthesis of Porphyrin-2,3,12,13- and −2,3,7,8-tetraones: Building Blocks for the Synthesis of Extended Porphyrin Arrays. *J. Chem. Soc., Chem. Commun.* **1995**, 2379−2380.

(23) Thordarson, P.; Marquis, A.; Crossley, M. J. The Synthesis and Studies Towards the Self-Replication of Bis(capped porphyrins). *Org. Biomol. Chem.* **2003**, *1*, 1216−1225.

(24) Collman, J. P.; Sunderland, C. J.; Boulatov, R. Biomimetic Studies of Terminal Oxidases: Trisimidazole Picket Metalloporphyrins. *Inorg. Chem.* **2002**, *41*, 2282−2291.

(25) Gouterman, M. Optical Spectra and Electronic Structure of Porphyrins and Related Rings. In *The Porphyrins*; Dolphin, D., Ed.; Academic Press: New York, 1978; Vol 3; pp 1−165.

(26) Karweik, D. H.; Winograd, N. Nitrogen Charge Distributions in Free-Base Porphyrins, Metalloporphyrins, and their Reduced Analogs Observed by X-Ray Photoelectron Spectroscopy. *Inorg. Chem.* **1976**, *15*, 2336−2342.

(27) Sakurai, T.; Yamamoto, K.; Naito, H.; Nakamoto, N. The Crystal and Molecular Structure of Chloro-$\alpha,\beta,\gamma,\delta$-tetraphenylporphinatocobalt(III). *Bull. Chem. Soc. Jpn.* **1976**, *49*, 3042−3046.

(28) Buttry, D. A.; Anson, F. C. New Strategies for Electrocatalysis at Polymer-Coated Electrodes. Reduction of Dioxygen by Cobalt Porphyrins Immobilized in Nafion Coatings on Graphite Electrodes. *J. Am. Chem. Soc.* **1984**, *106*, 59−64.

(29) Song, E.; Shi, C.; Anson, F. C. Comparison of the Behavior of Several Cobalt Porphyrins as Electrocatalysts for the Reduction of O_2 at Graphite Electrodes. *Langmuir* **1998**, *14*, 4315−4321.

(30) Lysenko, A. B.; Thamyongkit, P.; Schmidt, I.; Diers, J. R.; Bocian, D. F.; Lindsey, J. S. Diverse Porphyrin Dimers as Candidates for High-Density Charge Storage Molecules. *J. Porphyrins Phthalocyanines* **2006**, *10*, 22−32.

(31) Lennox, J. C.; Murray, R. W. Chemically modified electrodes. 10. Electron Spectroscopy for Chemical Analysis and Alternating Current Voltammetry of Glassy Carbon-Bound Tetra(aminophenyl)-porphyrins. *J. Am. Chem. Soc.* **1978**, *100*, 3710−3714.

(32) Rocklin, R. D.; Murray, R. W. Chemically modified carbon electrodes: Part XVII. Metallation of Immobilized Tetra-(aminophenyl)porphyrin with Manganese, Iron, Cobalt, Nickel, Copper and Zinc, and Electrochemistry of Diprotonated Tetraphenylporphyrin. *J. Electroanal. Chem. Interfacial Electrochem.* **1979**, *100*, 271−282.

(33) Jester, C. P.; Rocklin, R. D.; Murray, R. W. Electron Transfer and Axial Coordination Reactions of Cobalt Tetra(Aminophenyl)-Porphyrins Covalently Bonded to Carbon Electrodes. *J. Electrochem. Soc.* **1980**, *127*, 1979−1985.

(34) Rosenthal, J.; Nocera, D. G. Role of Proton-Coupled Electron Transfer in O−O Bond Activation. *Acc. Chem. Res.* **2007**, *40*, 543−553.